Catalysis Today 137 (2008) 197–202

Contents lists available at ScienceDirect

Catalysis Today

journal homepage: www.elsevier.com/locate/cattod

Adsorption and interaction of NO, C_3H_6 and O_2 on Pt, Zr, Nb-MCM-41—FTIR study

J. Goscianska, M. Ziolek *

Adam Mickiewicz University, Faculty of Chemistry, Grunwaldzka 6, 60-780 Poznan, Poland

ARTICLE INFO

Article history:
Available online 15 May 2008

Keywords:
Zr
NbMCM-41 supports for platinum
Texture/structure
NO + O_2 + C_3H_6-FTIR

ABSTRACT

Adsorption of NO, O_2 and C_3H_6 on the MCM-41 matrices with Nb and Zr loaded with Pt has been studied by the FTIR spectroscopy to characterize these materials as catalysts in the selective reduction of NO with propene. Two types of the catalysts have been studied differing by the methods of Zr and Nb introduction: either by one-pot (group 1) or by post-synthesis impregnation (group 2) and hence by the location of Nb and Zr in the framework (group 1) or extra framework (group 2). It has been found that the positions of these metals in the MCM-41 matrix determine the platinum dispersion, acidic–basic properties and influence the interaction of NO + O_2 + C_3H_6 with the catalyst surfaces. The fact that the Pt dispersion is much higher in group 2 materials has been revealed by results of XRD patterns and TEM images. According to the explanation proposed, the presence of Lewis acid–base pairs in the group 2 of catalysts has strongly activated chemisorption of propene, whereas Lewis basicity, characterized by 2-PrOH dehydrogenation on the samples containing transition metals introduced during the synthesis (group 1), has enhanced chemisorption of nitrite species on platinum. It has been proved that nitrite species have not been stored on Pt/Zr/MCM-41 samples, whereas they have been stabilized on Pt/Zr/Nb/MCM-41 containing BrØnsted acidic centres.

1. Introduction

Recently, mesoporous MCM-41 materials have been used as supports for Pt [1–6] and applied in HC–SCR of NO_x (e.g. [6,7]). Shen and Kawi [7] applied Pt/MCM-41 in this process, and they have found that the adsorption and activation of hydrocarbon is an important step for NO reduction. With the use of Pt/MCM-41 hydrocarbon reaction pathway was noted. The object of our interest was the NbMCM-41 matrix which appeared to be an attractive Pt support because of possible NO_x storage effect on niobium species [1,4,6]. The presence of niobium in the NbMCM-41 matrix enhances the oxidative properties of the catalysts [8]. NO is oxidized on NbO^- species present on the catalyst and stored in the form of nitrite/nitrate species [6]. This material (Pt/NbMCM-41) could be used as the so-called NSR (NO storage reduction) catalyst but the chemisorption of nitrate/nitrite intermediates is too strong. The NSR catalyst is based on alumina supported platinum material doped with barium playing the role of the NO_x storage agent. However, barium is easily poisoned by sulphur dioxide, whereas niobium species in NbMCM-41 material do not interact with SO_2 so strongly.

In fact, the role of nitrate species as true reaction intermediates in the SCR process over oxides has been indicated by many research teams and pointed out in the review paper by Burch et al. [9]. The formation of ad-NO_x species on the catalyst surface was proposed to be the first reaction step. For further reaction with the reductant (hydrocarbon), during the rich fuel cycle, the possibility of nitrates decomposition is important. Sadykov et al. [10] showed that the decomposition temperatures of strongly bound ad-NO_x species corresponded well to the onset of propane–SCR activity over many catalysts studied. For alumina and Ag/alumina, Shimizu et al. [11,12] proved that nitrate species were converted to nitrogen upon exposure to the reductant at the rates that were similar to those of steady-state reduction of NO [9]. All these results can support the NO reaction pathway for the SCR process. However, it should be noted that the ad-NO_x species are easier formed from NO_2. Therefore, the catalysts that activate NO oxidation to NO_2 facilitate the formation of nitrates. The high rate of NO_2 (g) formation is clearly related to the high activity in hydrocarbon combustion [9]. Thus, it can happen that the catalysts active for the oxidation of NO are unselective for the SCR reaction, as indicated by Meunier et al. [13] for Co/alumina catalysts.

In our recent FTIR study of NO, C_3H_6 and O_2 co-adsorption and interaction on Pt/NbMCM-41 materials, we have established nitrate formation on niobium species but they were too strongly bound to the surface, which made a further reaction with propene impossible [6]. Therefore, in this work we have prepared new

* Corresponding author. Tel.: +48 61 8291243; fax: +48 61 865 80 08.
E-mail address: ziolek@amu.edu.pl (M. Ziolek).

0920-5861/$ – see front matter © 2008 Elsevier B.V. All rights reserved.
doi:10.1016/j.cattod.2008.04.002

compositions of the mesoporous matrices, on which platinum was loaded and contrary to our earlier studies, the samples were reduced in hydrogen flow. The latter could change not only the platinum oxidation state but also that of niobium and maybe zirconium. Although Zr-oxides are commonly assumed non-reducible, recently [14] the reducibility of ZrO_2 has been detected. We have expected that the introduction of zirconium near niobium species in MCM-41 matrix will weaken the bonding of nitrates on niobium species and enhance the SCR selectivity. The aim of this paper was to study the NO + C_3H_6 + O_2 adsorption, co-adsorption and interaction on Pt/ZrNbMCM-41 catalysts by *in situ* FTIR spectroscopy. Prior to these studies the catalysts were characterized by the test reactions (2-propanol decomposition and acetonylacetone cyclisation) for the estimation of acidic–basic and redox properties, important for SCR process. For instance, BrØnsted acidity is required in some steps of the proposed mechanism for SCR of NO with propane on Ag exchanged MFI zeolites [15]. Lewis acid–base pairs are important in the activation of hydrocarbons (e.g. methane in [16]). Moreover, the texture/structure of the materials was characterized by XRD, N_2 adsorption, and TEM measurements.

2. Experimental

2.1. Samples preparation—synthesis and modification

MCM-41 was synthesized by the hydrothermal method from sodium silicate (27% SiO_2 in 14% NaOH; Aldrich) and cetyltrimethylammonium chloride (25 wt.% in water; Aldrich) as a template. Trisoxalate ammonium complex of niobium (CBMM, Brazil) and $ZrO(NO_3)_2$ (Alfa Aesar) were used for mono and bimetallic silicates production. The Si/T atomic ratio (T=Nb and/or Zr) in the gels was between 10 and 128 (Table 1). So prepared Nb(128)MCM-41, Zr(128 or 10)MCM-41 and MCM-41 were impregnated by the aqueous solution of Zr and Nb salt, respectively, to receive the Si/metal molar ratio equal to 128.

All the materials were impregnated by the incipient wetness technique with aqueous solution of chloroplatinic acid–$H_2PtCl_6 \times H_2O$ (Aldrich) in the concentration that corresponded to 1 wt.% Pt loading. The catalysts were successively dried at 363 K for 5 h (temperature ramp 3 K min^{-1}) and calcined at 773 K for 3 h (temperature ramp 2 K min^{-1}) in air, then reduced in H_2 (5 vol.% H_2/N_2) at 773 K for 3 h (temperature ramp 2 K min^{-1}).

2.2. Samples characterization

The prepared materials were characterized by XRD (TUR-62 diffractometer, Cu Kα radiation (λ = 0.154 nm). The surface area and pore volume of the MCM-41 materials were estimated by nitrogen adsorption at 77 K using the conventional technique on a Micromeritics 2010 apparatus. Prior to the adsorption measurements, the samples were degassed in vacuum at 573 K for 2 h. For TEM measurements powders were deposited on a grid with a holey carbon film and transferred to JEOL 2000 electron microscope operating at 80 kV.

2.3. 2-Propanol decomposition—test reaction

The materials prepared were tested in 2-propanol decomposition as a probe reaction. The 2-propanol decomposition is a test reaction for the characterization of acidic (BrØnsted or Lewis) and/or basic properties of solids [17]. Dehydration of alcohol to propene and/or di-isopropyl ether requires acidic centres (Lewis or BrØnsted), whereas the dehydrogenation to acetone occurs on basic sites. It is noteworthy that ether production requires the presence of pairs Lewis acid–base centres. Some authors (e.g. [18]) have stated that acetone formation takes place on redox centres. So, this probe reaction allows the estimation of acidic, basic and redox properties of the catalysts.

The 2-propanol (Aldrich) conversion (dehydration and dehydrogenation) was performed using a micro pulse reactor inserted between the sample inlet and the column (Carbowax 400) of a CHROM-5 chromatograph (TCD detector). The catalyst bed (0.02 g) was first activated at 673 K for 2 h under helium flow. The reaction was studied at the range 423–673 K using 5 μl pulses of alcohol under helium flow (40 cm^3 min^{-1}). Three pulses were introduced at each temperature.

2.4. Acetonylacetone cyclisation/dehydration—test reaction

The materials were tested in acetonylacetone (AcAc) cyclisation as a probe reaction. A tubular, down-flow reactor was used in experiments carried out at atmospheric pressure, using nitrogen as a carrier gas. The catalyst bed (0.05 g) was first activated for 2 h at 673 K under nitrogen flow (40 cm^3 min^{-1}). Afterwards, a 0.5 cm^3 of acetonylacetone (Fluka, GC grade) was passed continuously over the catalyst at 623 K. The substrate was delivered with a pump system and vaporized before it was passed through the catalyst bed in the presence of a flow of nitrogen carrier gas (40 cm^3 min^{-1}). Reaction products were collected during 30 min downstream of the reactor in the cold trap (solid CO_2) and analysed by gas chromatography (GC 8000 Top equipped with a capillary column of DB-1, operated at 353 K, attached to a FID).

2.5. Samples FTIR characterization—DeNO$_x$ study

Infrared spectra were recorded with the Vector 22 (Bruker) spectrometer. The pressed wafers of the materials (~10 mg cm^{-1}) were placed in the vacuum cell and activated at 673 K for 3 h under vacuum (0.04 mbar). After such activation the reagents ($NO:O_2:C_3H_6$, 1:1:1) were subsequently admitted at room temperature (RT) and FTIR spectra were recorded. The experiments were carried out in static conditions. The spectra were also measured after heating the samples at 373, 473 and 573 K for 0.5 h at each temperature. The spectrum without the sample (“background spectrum”) after the reagents admission (gas phase

Table 1
Characteristic of MCM-41 materials used in this work

Catalyst[a]	S (m^2/g), BJH ads.	Mesopore diam., D (nm), from PSD	V total (cm^3 g^{-1})	Wall thickness[b], t (nm)
Pt/Nb(128)MCM-41	906 ± 2.3	2.83	1.32	1.76
Pt/Zr(128)MCM-41	776 ± 1.7	2.03	0.72	2.26
Pt/Zr(10)MCM-41	352 ± 1.4	2.01	0.72	2.38
Pt/Zr(128)/MCM-41	1099 ± 5.8	3.07	0.69	1.82
Pt/Zr(256)/Nb(256)/MCM-41	1162 ± 6.3	3.58	0.86	1.86

[a] The numbers in brackets indicate Si/metal molar ratio; slash stands for the impregnation method.
[b] $t = a_0 - D/1.05$.

spectrum) was subtracted from all recorded spectra. So, the presented spectra are those of the catalyst surface after the subtraction of the gas phase. Moreover, the IR spectra of the activated samples were subtracted from those recorded after the adsorption of molecules followed by various treatments.

3. Results and discussion

The samples, after synthesis, were analysed from the point of view of structural, textural and morphological properties. Nitrogen adsorption isotherms of all the materials studied are of type IV (characteristic of mesoporous materials) according to the IUPAC classification.

Fig. 1A shows the X-ray diffraction patterns at a low-angle range characteristic of the mesostructured materials with highly ordered hexagonal arrangement [19]. They are characterized by a narrow single Bragg peak (1 0 0) at $2\theta \sim 2^\circ$ and up to three peaks in the region of $2\theta \sim 3$–8°.

Table 1, exhibiting texture/structure parameters of all materials used in this study, clearly indicates that these features significantly depend on the chemical composition of the support and the methods and the amount of zirconium and niobium loading. Zr introduced during the synthesis of MCM-41 leads to high wall thickness (calculated assuming the hexagonal pore geometry and the unit cell parameter, a ($a = 2(3^{-1/2})d$), minus the distance between the midpoints of the sides of the hexagonal cross section (equal to $D/1.050$) [20]) and small mesopore diameter and BJH surface area. The increase in Zr content causes the growth of wall thickness and decrease in pore diameter. This feature is less noted if Zr is introduced into niobiosilicate MCM-41 matrix. Interestingly, the materials in which Zr and/or Nb were loaded on silicate MCM-41 via wet impregnation are characterized by high surface areas (above 1000 m^2/g) and pore diameters (above 3 nm) as well as relatively small (below 2 nm) wall thickness.

The above results prove that zirconium is located in the skeleton of the MCM-41 matrix replacing of Si, leading to change the texture parameters. The other proof for that statement has been shown in [2] on the basis of the UV–vis spectra (the band at ca 230 nm from tetrahedrally coordinated zirconium [21,22]). The texture/structure characteristic of the supports has a very high impact on the platinum dispersion. The highest surface area and mesopore diameter noted for Pt/Zr(256)/Nb(256)/MCM-41 result

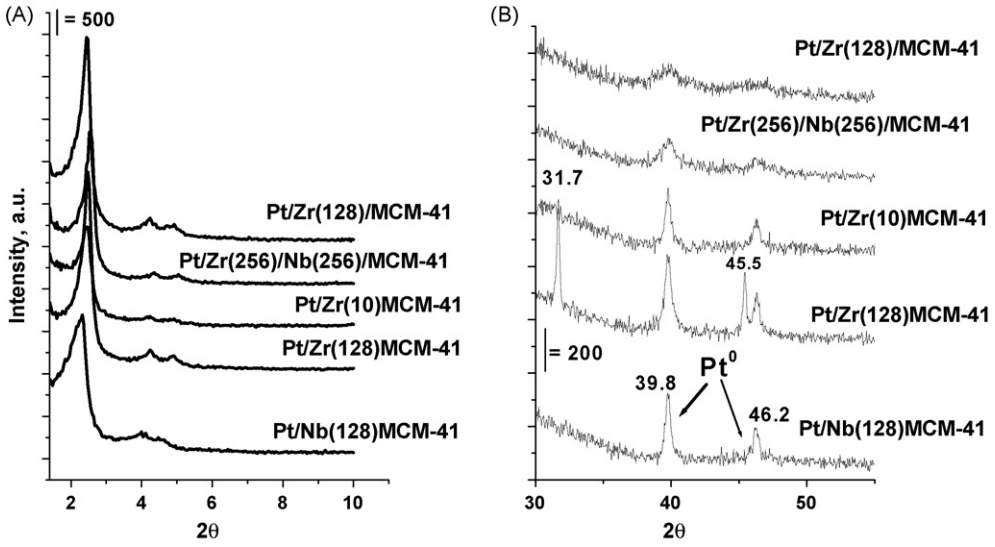

Fig. 1. Small-angle (A) and high-angle (B) X-ray diffraction patterns of MCM-41 materials.

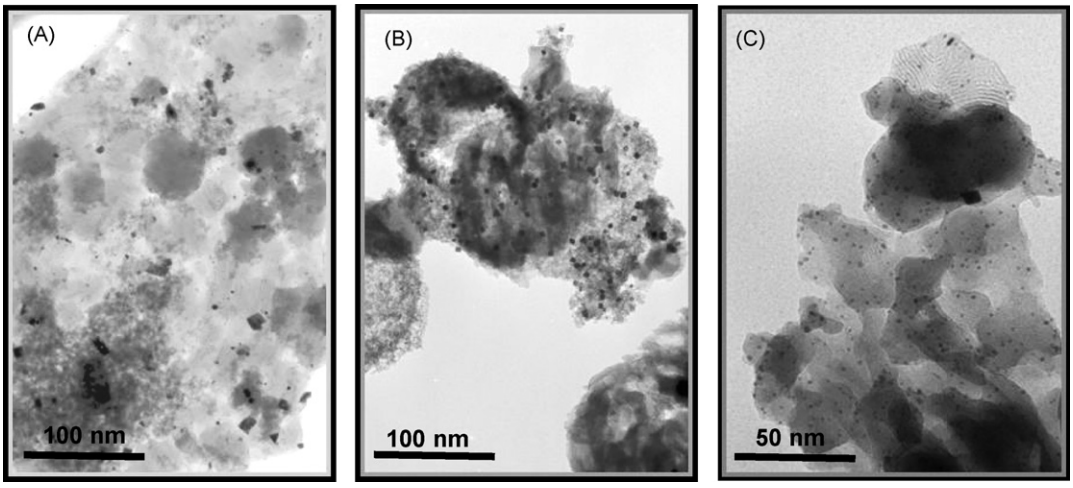

Fig. 2. TEM micrographs of Pt/Nb(128)MCM-41 (A), Pt/Zr(128)MCM-41 (B), and Pt/Zr(256)/Nb(256)/MCM-41 (C).

Table 2
Results of 2-propanol (2-PrOH) decomposition at 523 K and acetonylacetone (AcAc) cyclisation at 623 K

Catalyst	2-PrOH				AcAc	
	Conv.[a] (%)	Propene select. (%)	Acetone select. (%)	Ether select. (%)	Conv.[a] (%)	MCP/DMF[b]
Pt/Nb(128)MCM-41	3	100	–	–	13	1.1
Pt/Zr(128)MCM-41	24	1	99	–	18	6.1
Pt/Zr(10)MCM-41	10	2	98	–	20	15.4
Pt/Zr(128)/MCM-41	28	69	27	–	29	1.5
Pt/Zr(256)/Nb(256)/MCM-41	26	2	98	4	32	0.3

[a] Error in measurement of conversion is ±1%.
[b] MCP = methylcyclo-pentenone, DMF = dimethylfuran.

in the highest platinum dispersion well seen in TEM images (Fig. 2) and confirmed by a high-angle XRD pattern (Fig. 1B). Moreover, zirconium and niobium species located on the walls (not inside) in the impregnated samples play the role of a structural promoter which decreases the agglomeration of platinum.

The presence of Pt-metal clusters is evidenced in the high-angle range of the XRD patterns (Fig. 1B). The characteristic reflections of metallic platinum at 39.7° ((1 1 1) plane) and 46.2° ((2 0 0) plane) [7,25] are well visible for Pt/Nb(128)MCM-41, Pt/Zr(128)MCM-41, and Pt/Zr(10)MCM-41, whereas for Pt/Zr(256)/Nb(256)/MCM-41 and Pt/Zr(128)/MCM-41 samples both peaks are wide and of low intensity indicating a high platinum dispersion. The XRD pattern of Pt/Zr(128)MCM-41 shows additional peaks at 2θ of 31.7° and 45.5° (Fig. 1B). The reflections at 31.7° and 45.5° can be indexed to the ZrSi (1 1 1) – JCPDF file 72-1271, ZrO_2 (2 1 1) – JCPDF file 86-1451, respectively [2].

The question arises whether the texture/structure behaviour of the prepared samples influences the catalytic properties of the surface. The redox/basic properties of all the materials are strongly evidenced by the acetone formation in 2-PrOH reaction (Table 2),

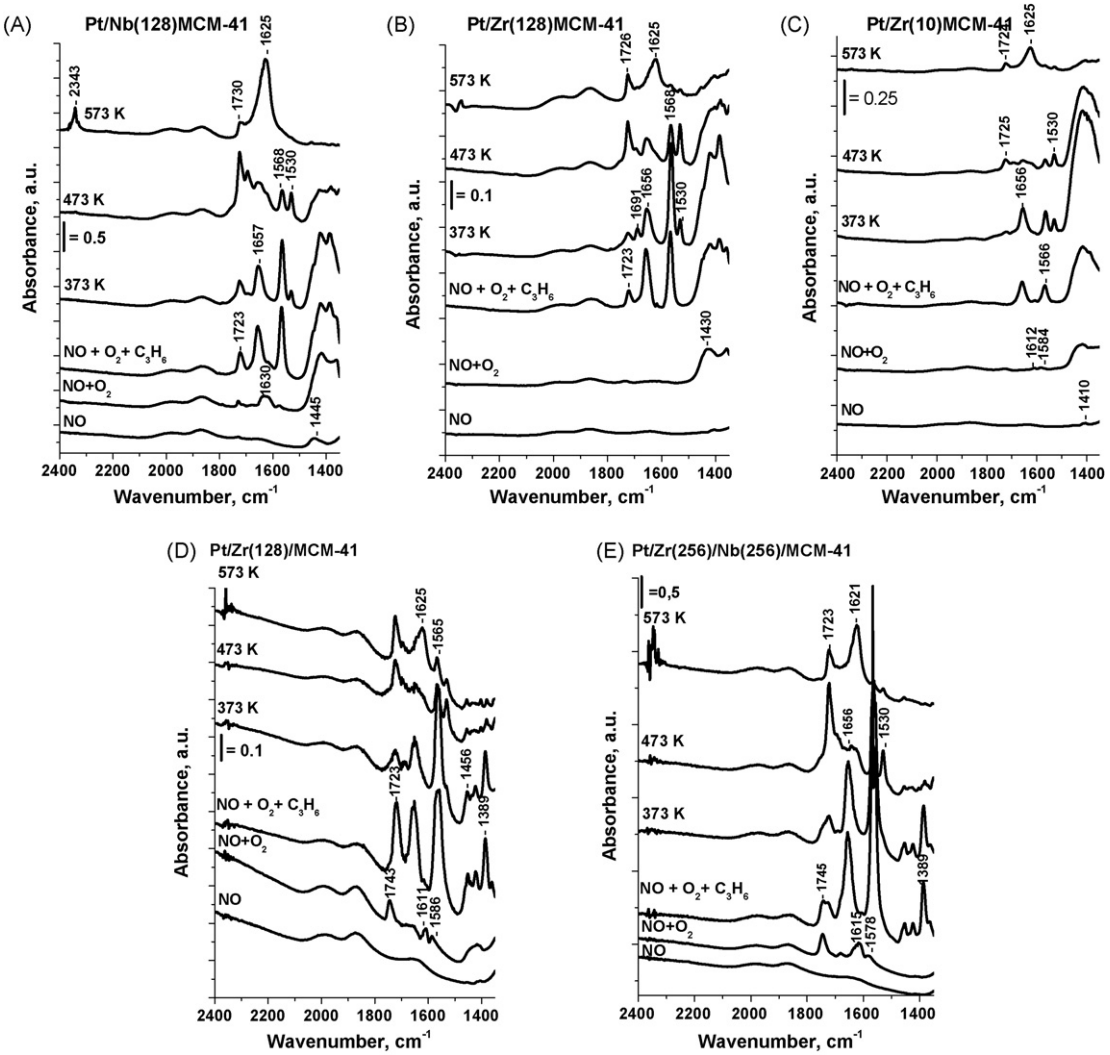

Fig. 3. FTIR spectra of the catalyst surface (after the subtraction of the spectra of gas phase and the activated sample): Pt/Nb(128)MCM-41 (A), Pt/Zr(128)MCM-41 (B), Pt/Zr(10)MCM-41 (C), Pt/Zr(128)/MCM-41 (D), and Pt/Zr(256)/Nb(256)/MCM-41 (E) after the adsorption of 0.5 mbar of NO, O_2 and C_3H_6 at room temperature and next heating for 30 min at 373, 473, and 573 K.

and they depend on the nature of the support. If one compares the results obtained over the Pt/Zr(128)MCM-41 and Pt/Zr(128)/MCM-41 samples (i.e. two various supports: one possessing Zr in the skeleton and the other in which Zr is in the extra framework position, most probably in the form of zirconium oxide), the role of Zr location is clearly seen. Zirconium introduced by the impregnation (located in the extra framework sites) significantly decreases the acetone formation by increasing the acidity of the surface (propene production). Pt/Nb(128)MCM-41 exhibits the acidic character (100% selectivity to propene), whereas diisopropyl ether is formed only when both transition metals (Nb and Zr) are included, showing that pairs of acid–base centres are present.

Interestingly, the results of 2-propanol decomposition well correlate with most of the results from the second test reaction: acetonylacetone cyclisation. It is known [23,24] that in this reaction dimethylfuran (DMF) is produced on Brønsted acid centres, whereas Brønsted basic centres are involved in the formation of methylcyclo-pentenone (MCP). It is known that the selectivities MCP/DMF $\gg 1$ characterize basic properties of the catalyst, whereas MCM/DMF $\ll 1$ indicates the acidic character of the material. If this ratio is $\sim$1, the acidic–basic character of the catalyst can be concluded. The data in Table 2 show that, like in 2-PrOH reaction, the reaction route involving basic centres (MCP/DMF $\gg 1$) dominates on both samples in which Zr was introduced by co-precipitation during the synthesis of MCM-41. For the other two samples, Pt/Nb(128)MCM-41 and Pt/Zr(128)/MCM-41, the results of both test reactions are also in agreement. However, the difference is evidenced for Pt/Zr(256)/Nb(256)/MCM-41, which reveals the acidic character in the AcAc reaction whereas the basic one in 2-PrOH dehydrogenation. One should point out that in acetonylacetone transformation towards MCP, Brønsted basic centres are involved, whereas acetone is formed from 2-PrOH on Lewis basic sites. That explains the difference in the results for both test reactions and indicates that Pt/Zr(256)/Nb(256)/MCM-41 exhibits Lewis basicity and Brønsted acidity on the surface.

The difference in the adsorption and interaction between NO and C_3H_6 in the presence of oxygen is observed, depending on the chemical composition of the matrix for Pt and the way of transition metal loading, which determine the structure and surface properties as indicated above. Upon NO adsorption at RT, the only species observed in FTIR spectra (Fig. 3) is monodentate nitrito one [16] (a band at 1445 or 1410 cm^{-1} depending on the composition of the matrix). This band is the most pronounced in the spectrum of Pt/Nb(128)MCM-41. The following admission of oxygen leads to a significant increase in the intensity of these bands for the materials with a lower Pt dispersion, i.e. those whose matrices contain Zr or Nb in the skeleton (Fig. 3A–C). This behaviour shows that such materials contain sites which can play the role of NO_x traps. Such sites are not observed on Pt/Zr(256)/Nb(256)/MCM-41 (Fig. 3E) which indicated BrØnsted acidity in acetonylacetone cyclisation (Table 2). However, on this material, as well as on Pt/Zr(128)/MCM-41 (both showing a high Pt dispersion) the admission of NO + oxygen results in the chemisorption of NO_2^- on Pt (the band at 1745 cm^{-1}) and gives also the bands at 1612 and 1578 cm^{-1} which can be assigned to bridged bidentate nitrates and bidentate nitrates bonded to zirconium cations, respectively [16,26]. Pt–NO_2^- species are not formed on Pt/Zr(128)MCM-41 and Pt/Zr(10)MCM-41 (the materials where Zr is located in the framework), most probably because of the interaction of Pt with the bridged oxygen in Zr–O–Si inside the walls of the mesoporous matrix.

After the following admission of propene at RT, the difference between Pt/Zr(128)/MCM-41 and Pt/Zr(256)Nb(256)/MCM-41 is clearly seen (Fig. 3D and E). For the first material, NO_2^- chemisorbed on Pt (1743 cm^{-1}) disappears suggesting the reaction with hydrocarbon, whereas for the second sample this band is still present and disappears after heating at 573 K. It can indicate that BrØnsted acid centres, determined by the AcAc reaction on Pt/Zr(256)Nb(256)/MCM-41, stabilize NO_2^- adsorbed on Pt species.

For all the samples studied, the adsorption of propene led to the appearance of the IR bands in the 1300–1500 cm^{-1} region from ν =CH_2 and =CH characteristic of physisorbed and weakly chemisorbed propene. These bands are more pronounced in the spectra of the samples with a higher platinum dispersion (Fig. 3D and E). For the other three catalysts these bands are overlapped with that assigned to nitrite species. Moreover, after propene adsorption three main bands appear in the range 1500–1750 cm^{-1}. There are bands at $\sim$1570 cm^{-1} assigned to acetates [27,28], $\sim$1656 cm^{-1} assigned to organic nitrito compound (C_3H_7–ONO) [29,30], and at $\sim$1723 cm^{-1} assigned to C=O in acetone [31]. These intermediates give the most intensive IR bands in the spectra of the samples with the highest Pt dispersion (Fig. 3D and E) and the weakest bands in the spectrum of Pt/Zr(10)MCM-41 because of a too high concentration of zirconium.

Heating of the catalysts with the adsorbed species causes a typical, described in many papers (e.g. [5,6,9,16,26,29,30]), transformation of acetates (1570 cm^{-1}) to carbonates ($\sim$1530 cm^{-1}) [31] and organic nitrito compound (1656 cm^{-1}) to acetone (1723 cm^{-1}). The highest intensity of the band assigned to acetone was observed after heating at 473 K, in the spectra of the majority of samples (with the exception of Pt/Zr(128)/MCM-41). Finally, heating at 573 K leads to the formation of water and carbon dioxide.

4. Conclusions

Platinum is much better dispersed on the MCM-41 matrices in which Zr and Nb are introduced via the impregnation, i.e. they are located in the extra framework positions. The location of Zr and/or Nb has a significant impact also on the NO + O_2 interaction with the catalyst surface. Nitrite species are formed much easier on the catalysts based on the matrices containing Zr or Nb introduced during the synthesis, whereas they are not formed on the impregnated sample in which Zr and Nb are located in the extra framework position. Post-synthesis impregnation with Zr and/or Nb, and Pt loading gives rise to the catalysts which adsorb NO + O_2 mixture in the form of NO_2^- chemisorbed on platinum species. This form is not stored and it is active towards C_3H_6 at room temperature on Pt/Zr(128)/MCM-41 but is stabilized on Pt/Zr(256)/Nb(256)/MCM-41 containing BrØnsted acidic centres. The presence of Lewis acid–base pairs in both above mentioned samples strongly activates chemisorption of propene, whereas Lewis basicity, characterized by 2-PrOH dehydrogenation on the samples containing transition metals introduced during the synthesis, enhances chemisorption of nitrite species.

Acknowledgements

Polish Ministry of Science and Higher Education (grant no. N N204 3735 33) and CBMM (Brazil) are acknowledged for the financial support and for the supplying Nb source, respectively.

References

[1] P. Broqvist, H. Grönbeck, E. Fridell, I. Panas, Catal. Today 96 (2004) 71.
[2] J. Goscianska, M. Ziolek, Stud. Surf. Sci. Catal. 165 (2007) 215.
[3] J. Goscianska, M. Ziolek, Stud. Surf. Sci. Catal. 170B (2007) 1870.
[4] J. Goscianska, M. Ziolek, Pol. J. Environ. Stud. 15 (2006) 53.
[5] I. Sobczak, M. Ziolek, M. Nowacka, Microporous Mesoporous Mater. 78 (2005) 103.
[6] J. Goscianska, Ph. Bazin, O. Marie, M. Daturi, I. Sobczak, M. Ziolek, Catal. Today 119 (2007) 78.
[7] S.C. Shen, S. Kawi, Appl. Catal. B: Environ. 45 (2003) 63.

[8] M. Ziolek, I. Sobczak, A. Lewandowska, I. Nowak, P. Decyk, M. Renn, B. Jankowska, Catal. Today 70 (2001) 169.
[9] R. Burch, J.P. Breen, F.C. Meunier, Appl. Catal. B: Environ. 39 (2002) 283.
[10] V. Sadykov, S.L. Baron, V.A. Matyshak, G.M. Alikina, R.V. Bunina, A.Y. Rozovskii, V.V. Lunin, E.V. Lunina, A.N. Kharlanov, A.S. Ivanova, S.A. Veniaminov, Catal. Lett. 37 (1996) 157.
[11] K. Shimizu, J. Shibata, H. Hyoshida, A. Satsuma, T. Hattori, Appl. Catal. B 30 (2001) 151.
[12] K. Shimizu, J. Shibata, A. Satsuma, T. Hattori, Phys. Chem. Chem. Phys. 3 (2001) 880.
[13] F.C. Meunier, V. Zuzaniuk, J.P. Breen, M. Olsson, J.R.H. Ross, Catal. Today 59 (2000) 287.
[14] I. Dobrosz, Ph.D. Thesis, Technical University of Lodz, 2007.
[15] K. Shimizu, K. Sugino, K. Kato, S. Yokota, K. Okumura, A. Satsuma, J. Phys. Chem. C 111 (2007) 6481.
[16] M. Kantcheva, A.S. Vakkasoglu, J. Catal. 223 (2004) 364.
[17] A. Gervasisni, J. Fenyvesi, A. Auroux, Catal. Lett. 43 (1997) 219.
[18] C. Lahausse, J. Bechelier, J.C. Lavalley, H. Lauron-Pernot, A.M. Le Govic, J. Mol. Catal. 87 (1994) 329.
[19] J.S. Beck, J.C. Vartuli, W.J. Roth, M.E. Leonowicz, D.T. Kresge, K.D. Schmitt, C.T.W. Chu, D.H. Olson, E.W. Sheppard, S.B. McCullen, J.B. Higgins, J.L. Schlenker, J. Am. Chem. Soc. 114 (1992) 10834.
[20] M. Kruk, M. Jaroniec, A. Sayari, J. Phys. Chem. B 101 (1997) 583.
[21] T. Onfroy, G. Clet, M. Houalla, J. Phys. Chem. B 109 (2005) 3345.
[22] T. Onfroy, G. Clet, M. Houalla, J. Phys. Chem. B 109 (2005) 14588.
[23] R.M. Dessau, Zeolites 10 (1990) 205.
[24] J.J. Alcaraz, B.J. Arena, R.D. Gillespie, J.S. Holmgren, Catal. Today 43 (1998) 89.
[25] J. Perez-Ramirez, J.M. Garcia-Cortes, F. Kepteijn, G. Mul, J.A. Moulijn, C. Salinas-Martinez de Lecea, Appl. Catal. B: Environ. 29 (2001) 285.
[26] K. Hadjiivanov, L. Dimitrov, Microporous Mesoporous Mater. 27 (1999) 49.
[27] W. Schießer, H. Vinek, A. Jentys, Appl. Catal. B: Environ. 33 (2001) 263.
[28] S.-C. Shen, S. Kawi, J. Catal. 213 (2003) 241.
[29] Y. Chi, S.S.C. Chuang, J. Catal. 190 (2000) 75.
[30] J.L. Valverde, A. de Lucas, F. Dorado, A. Romero, P.B. Garcia, J. Mol. Catal. A 230 (2005) 23.
[31] T.E. Hoost, K.A. Laframboise, K. Otto, Appl. Catal. B: Environ. 7 (1995) 79.